Behavior of a Mini Synthetic Jet in a Transverse Wall Flow: Experimental and Numerical Study — Source link ⎋

Ahmad Batikh, Lucien Baldas, Robert Caen, Stéphane Colin ...+2 more authors

Institutions: Institut national des sciences appliquées de Toulouse

Topics: Synthetic jet, External flow, Flow separation, Laminar flow and Open-channel flow

Related papers:

- Numerical and experimental study of mini synthetic jets actuators for flow control

- A Numerical Study on Internal and External flow fields of Synthetic Jet Actuator

- Experiments and Simulation of an Impinging Synthetic Jet Designed to Eliminate Actuator Artifacts

- Characterization of synthetic jet actuation with application to Ahmed body wake

- Numerical Investigation of the Behaviour of Circular Synthetic Jets for Effective Flow Separation Control

ICNMM2007-30103

BEHAVIOR OF A MINI SYNTHETIC JET IN A TRANSVERSE WALL FLOW: EXPERIMENTAL AND NUMERICAL STUDY.

**Ahmad BATIKH[1], Lucien BALDAS[1], Robert CAEN[1], Stéphane COLIN[1]
Azeddine KOURTA[2], Henri-Claude BOISSON[2]**

ahmad.batikh@insa-toulouse.fr, robert.caen@insa-toulouse.fr, stephane.colin@insa-toulouse.fr, lucien.baldas@insa-toulouse.fr
[1] LGMT-INSA, 135 Av. de Rangueil, 31077 Toulouse Cedex 4, France

kourta@imft.fr, henri.boisson@imft.fr
[2] Institut de Mécanique des Fluides de Toulouse, Allée du Prof. Camille Soula, 31400 Toulouse, France

ABSTRACT

A synthetic jet is a time-averaged fluid motion generated by sufficient strong oscillatory flow downstream from a sudden expansion. The study of the interaction between the synthetic jet and an external flow is of great interest in particular for aeronautical applications. A network of such actuators could be used indeed on airplane wings for example to control, with a good energetic efficiency, the boundary layer separation in order to increase the lift or the laminar / turbulent transition for drag reduction.

In this paper, the interaction of a sub-millimetric synthetic jet actuator with an external flow is experimentally studied. In these experiments, the actuation is ensured by acoustic excitations produced by a loud-speaker. Hot-wire anemometry is used for measurement of the velocity field in various functioning configurations (velocity of the transversal flow, actuation frequency,…). In most of the tested configurations, the boundary layer of the transversal flow is significantly modified by the synthetic jet, which shows that these types of actuators could be efficiently used for flow control purposes.

NOMENCLATURE

Symbol	Description	Unit
b	Local half width of the jet (based on half local central velocity)	m
C_μ	Momentum coefficient $C_\mu = \dfrac{\rho_j}{\rho_\infty} \dfrac{h}{D} \left[\dfrac{U_j}{U_\infty} \right]^2$	-
f	Membrane actuation frequency	Hz
h	Slot width	m
H_C	Cavity width	m
I_0	Average momentum injected per unit width during the ejection stage ($I_0 = \rho\, h \int_0^{T/2} u_0^2(t)\,dt$)	Kg.m²s⁻² Kg.m^{2}s^{-2}
l	Slot height	m
L_0	Jet "stroke length" ($L_0 = \int_0^{T/2} u_0(t)\,dt$)	m
L_C	Cavity height	m
Re_{Io}	Reynolds Number based on I_0. ($\mathrm{Re}_{Io} = \dfrac{\rho\, h \int_0^{T/2} u_0^2(t)\,dt}{\mu h}$)	-
Re_{Uo}	Reynolds Number based on the mean jet velocity and the slot width ($\mathrm{Re}_{Uo} = U_0 h/\nu = \rho U_0 h/\mu$)	-
s	Orifice outlet area	m^2
Sr	Strouhal Number ($Sr = St^2 / Re_{Uo}$)	-
St	Stokes Number ($St = \sqrt{2\pi f\, h^2/\nu}$)	-
T	Actuation period ($T = 1/f$)	s
U_∞	Freestream velocity	m s⁻¹
U_0	Time-averaged velocity at the orifice center during the ejection stage ($U_0 = L_0/T$)	m s⁻¹
$u_0(t)$	Instantaneous velocity at slot center	m s⁻¹
u_{cl}	Time-averaged velocity on the jet centerline	m s⁻¹
$u_{cl\,max}$	Maximum velocity on the jet centerline	m s⁻¹
u	Time-averaged local velocity	m s⁻¹
$U_{j\,max}$	Maximum velocity at the orifice center	m s⁻¹

μ	Dynamic viscosity	kg m^{-1}.s^{-1}
ν	Kinematic viscosity	m^2 s^{-1}
ρ	Density	kg m^{-3}

INTRODUCTION

Wall-bounded flows may be efficiently controlled by appropriately modifying the boundary layer structure. It is thus possible to reduce the drag or increase the lift of an aircraft wing, to favor mixing in a combustion chamber, to reduce the aero-acoustic noise or to improve heat transfer. The nature of perturbations that need to be introduced in the boundary layer mainly depends on the flow characteristics: Reynolds and Mach numbers, type of instabilities in the boundary layer… For high Reynolds numbers and for compressible flows, active control methods based on momentum injection in the near wall flow thanks to dynamic systems composed of sensors and actuators have proved to be more efficient that passive control devices which modify the boundary layer structure simply by changing the wall geometry (Gad el Hak, 1996), (Ho and Tai, 1998).

Several types of mechanical microactuators have been developed for active control applications (thermal microactuators, micro magnetic flaps, micro balloons…) (Batikh, *et al.*, 2004). However, many recent works have been devoted to fluidic solutions which have the advantage, important for reliability, to have no moving part in direct contact with the external flow and allow a simple control. Among those, the synthetic jet actuators (SJA) are composed of a cavity whose volume is modulated by a membrane itself activated by means of electrostatic or piezoelectric material, and an orifice (figure 1). When the membrane is moved, these actuators suck in, in the boundary layer, a certain amount of fluid of small momentum and reject this same amount of fluid with a larger momentum forming a vortex ring (in case of a circular orifice) or a pair of vortex (in case of a slot). If the vortices have a sufficient velocity to move outwards before the ejection of the next vortex, a train of vortices will be formed (Smith and Glezer, 1998). The created jet acts on the structures of the near wall flow and allows its control.
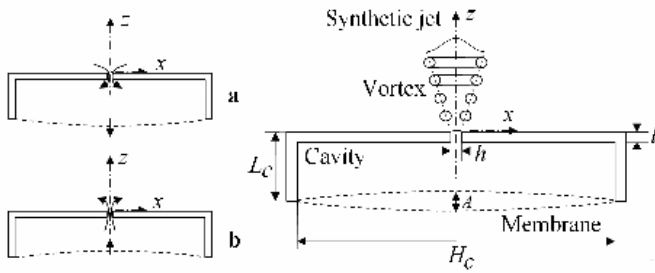

Figure 1. Principle of synthetic jet operation
a**.** aspiration, b**.** ejection

In order to characterize the synthetic jet behavior, several non-dimensional parameters may be considered:
- the jet *stroke length*

$$L_0 / h = \int_0^{T/2} u_0(t)\,dt / h \qquad (1)$$

permits to compare the ejection mean velocity with the actuation frequency; L_0 is the distance at which a fluid element moves away from the orifice during the ejection stage

(Utturkar, *et al.*, 2003), h is the orifice diameter or the slot width, T the actuation period and $u_0(t)$ the instantaneous velocity of jet at the center of the orifice/slot .

- viscosity effects are quantified by the Reynolds number which can be based:

- either on the average jet velocity U_0 at the center of the orifice/slot during the ejection stage and on the orifice/slot characteristic dimension h:

$$Re_{U_0} = U_0 h / \nu, \quad (2)$$

where ν is the kinematic viscosity and

$$U_0 = L_0 / T ; \qquad (3)$$

- or on the average momentum I_0 injected per unit width:

$$Re_{I_0} = I_0 / \mu h = \rho h \int_0^{T/2} u_0^2(t)\,dt . \quad (4)$$

For low *Reynolds* numbers, (typically for $Re_{U_0} < 50$), the flow does not separate from the orifice/slot edge during the ejection phase and the blowing and the suction phases are symmetrical.

- the *Stokes* Number

$$St = h / \delta_\nu = \sqrt{\omega h^2 / \nu} , \qquad (5)$$

where $\omega = 2\pi f$ and f is the membrane actuation frequency, compares the thickness of the unsteady boundary layer inside the orifice/slot to the orifice/slot characteristic length. For large Stokes numbers, viscosity does not affect the jet while for low St the unsteady boundary layer may limit significantly the jet average velocity.

- St and Re can also form a *Strouhal* number:

$$Sr = \frac{St^2}{Re} = \frac{\omega h^2 / \nu}{U_0 h / \nu} = \frac{\omega h}{U_0} = \frac{2\pi h / T}{L_0 / T} = 2\pi \frac{h}{L_0}. \quad (6)$$

This *Strouhal* number is inversely proportional to the stroke length defined by equation (1). For large *Strouhal* numbers, it will take several cycles for a fluid element to leave the orifice region, as for low *Sr* the fluid will cross this zone in only one cycle.

To sum up, with a *Reynolds* number rather low (low velocity, small orifice/slot or high kinematic viscosity), the fluid will be strongly influenced by viscosity effects at the orifice/slot. With a rather large *Strouhal* number (high frequency) the fluid will not have sufficient time to leave the orifice/slot during the compression phase. To generate strong jets with high momentum, it is thus necessary to operate the jet at high *Reynolds* number and low *Strouhal* number (Wu and Breuer, 2003).

When the synthetic jet actuator is used to control a cross flow, it is also useful to define the jet momentum coefficient (Traub, *et al.*, 2002)

$$C_\mu = \frac{\rho_j}{\rho_\infty} \frac{h}{D} \left[\frac{U_{j\,max}}{U_\infty} \right]^2 \qquad (7)$$

which will permit to quantify the synthetic jet efficiency, i.e. its capability to modify the cross flow structure. According to

previous studies (Seifert and Pack, 1999), the jet momentum must at least be on the order of 10^{-3} to have a substantial effect on the controlled cross flow. Note that this coefficient may also be defined using the root mean square of the velocity at the slot exit (Greenblatt, *et al.*, 2006).

In the first part of this paper, a sub-millimetric Synthetic Jet Actuator working in a quiescent air is experimentally and numerically characterized. The action of this actuator on a transverse wall flow is then studied experimentally. The first results obtained from numerical simulations of the synthetic jet in a cross flow are finally presented.

EXPERIMENTAL SETUP

The tested experimental SJA consists in a cylindrical cavity closed on one side by a metallic plate in which a rectangular slot has been machined and connected on the other side to the exit of a pneumatic signals generator. The latter is controlled (in frequency and amplitude) by an electric signals generator (figure 2-a) associated to a variable volume chamber.

The width and the length of the slot are 500 µm and 10 mm respectively. Its thickness is 500 µm. A pressure transducer (0.14×10^5 Pa maximum) is located on one side of the cavity and at 5 mm from the slot.
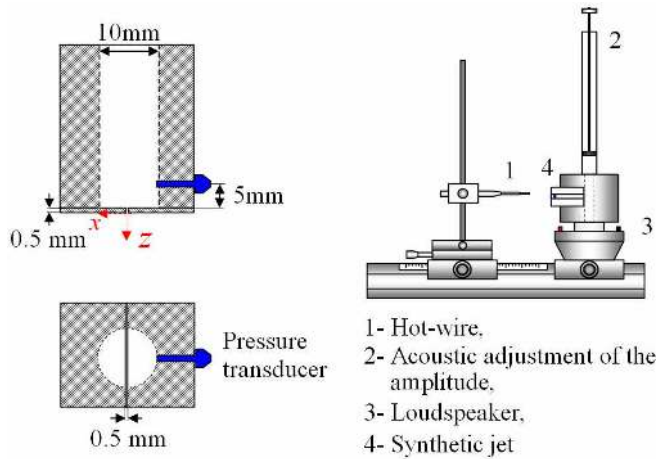
a. Synthetic jet system without external flow
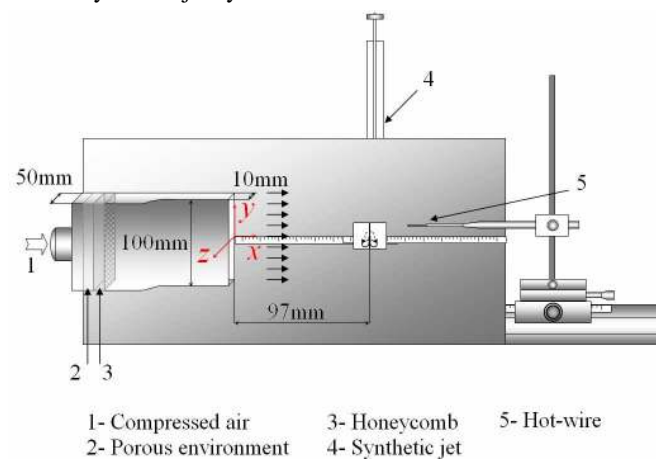
b. Synthetic jet system with cross flow

Figure 2. Experimental setup

In the second experimental configuration, (figure 2-b), the SJA is used to control a wall turbulent plane jet generated by a rectangular channel (10 mm height, 100 mm width) connected to a settling chamber via a converging element. A honeycomb flow straightener and a section of porous foam are installed between the chamber and the compressed air supplying pipe to ensure a low turbulence level and to produce a uniform, smooth flow.

The SJA is flush mounted on the plane plate, the slot center being at 97 mm from the channel exit (x direction) and the slot length in the same direction (noted y) than the channel width.

A single Dantec hot wire (9 µm in diameter) anemometer is used to measure the velocity. The signal of the hot wire is recorded on a computer via an acquisition card and software. The sampling rate is 10 kHz. The experimental standard deviation of the velocity measurements has been estimated, from the 4 measurements done at each probe location, to be of the order of 2.5%. It was mainly due to uncertainty in hot-wire calibration (±0.3%) and uncertainty in hot-wire probe position.

CHARACTERIZATION OF THE SYNTHETIC JET WITHOUT EXTERNAL FLOW

This study covers a frequency range from 50 to 1500 Hz and for each frequency a pressure peak to peak amplitude in the cavity between 2.5×10^2 and 2×10^3 Pa.
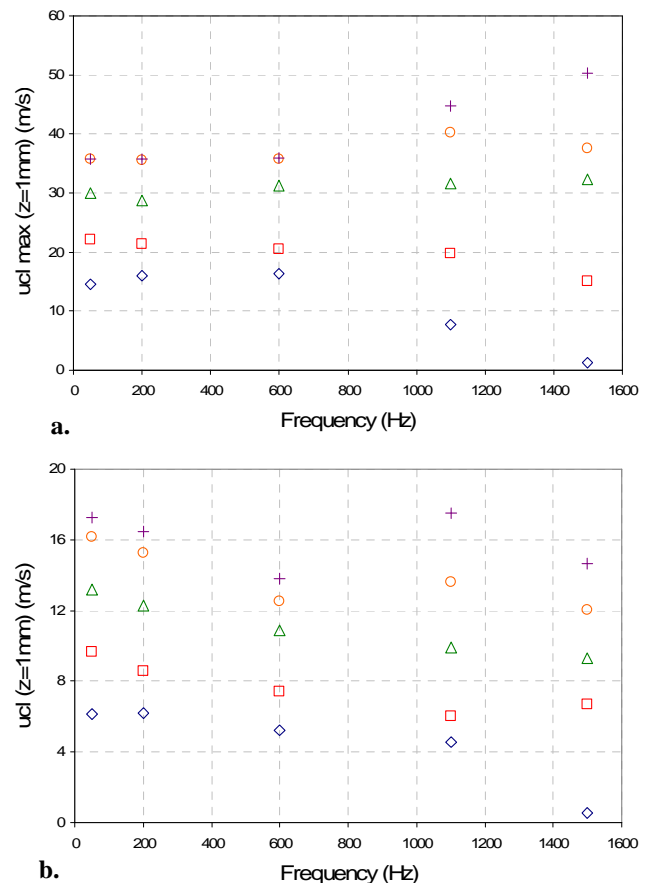

a.

b.

Figure 3. Variation of centerline velocity with frequency of SJ for z=1mm and for various pressure fluctuation amplitudes a. maximum velocity, b. time-averaged velocity
◇: 250 Pa, □: 500 Pa, △: 1000 Pa, ○: 1500 Pa, +: 2000 Pa

Once the jet symmetry has been checked, spanwise measurements are carried out at different distances from the slot on one side of the jet.

Figure 3 shows the evolution of the jet maximum centerline velocity and time-averaged (on one actuation period) centerline velocity at 1 mm from the slot exit plane with the actuation frequency and pressure amplitude in the cavity. For practical reasons, it was not possible to make measurements with the hot-wire probe closer from this plane. Whatever the actuation frequency, both maximum and time-averaged velocities are logically increasing with the pressure amplitude in the cavity. However, for low pressure amplitudes (250 Pa and 500 Pa), the maximum velocity on the centerline at the slot exit is rapidly decreasing for frequencies higher than 600 Hz. This "cutting" frequency does not seem to exist for higher pressure amplitudes, at least in the range of tested frequencies. On the contrary, for a pressure amplitude of 20 mbars, the maximum velocity increases with the frequency and reaches 50 m/s for f=50 Hz.

Time-averaged centerline velocity is slightly decreasing with the frequency for the three lowest pressure amplitudes, but a resonant frequency seems to exist around 1100 Hz for pressure amplitudes higher than 1500 Pa.
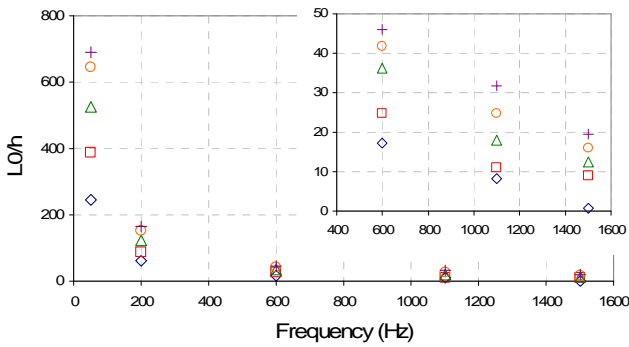

Figure 4. Variation of L_0/h with frequency
◇: 250 Pa, □: 500 Pa, △: 1000 Pa, ○: 1500 Pa, +: 2000 Pa

However, the SJA efficiency is not only function of its velocity but also depends on its capability to inject momentum in the cross flow. This can be evaluated through the jet stroke length L_0/h. This parameter is strongly decreasing when the frequency increases, showing that for frequencies higher than a few hundreds Hz, the reached ejection velocities are not high enough to let enough fluid leave the orifice region during the blowing phase (figure 4). In our case, according to this parameter, the lowest frequencies are so the most efficient ones even if higher peak jet speeds are reached for high frequencies. In the following part of this experimental study, the 200 Hz actuation frequency will thus be chosen.

Figure 5 shows the time-average velocity distributions along the jet axis. The velocity is scaled by its value on the centerline at 1 mm from the slot exit plane. The displacement along the jet axis is scaled by the slot width h.

All data for various pressure amplitudes roughly join on a single curve showing that the jet centerline mean velocity decays like $1/z^{0.5}$ (as in conventional turbulent jets) as shown by Kral (Kral, *et al.*, 1997).
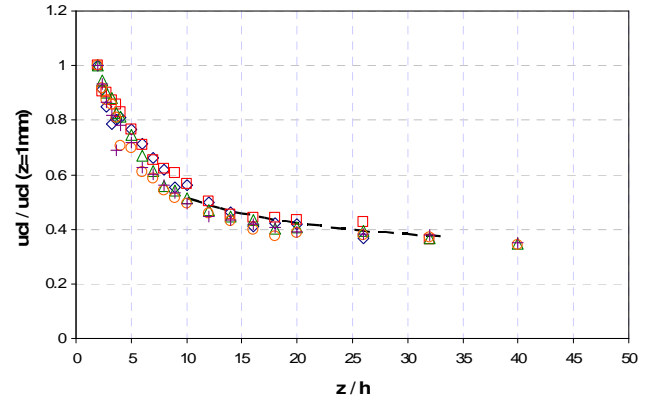

Figure 5. Distribution of time-averaged centerline velocity for f=200Hz
◇: 250 Pa, □: 500 Pa, △: 1000 Pa, ○: 1500 Pa, +: 2000 Pa,
---: $1/\sqrt{z}$

Figure 6 shows the transversal distribution of maximum velocity at three levels above the slot exit plane (z=1, 2 et 3 mm). The spanwise x-coordinate is normalized by the slot width h and the velocity by the centerline maximum velocity at z=1 mm.

In the three cases and for each pressure amplitude, classical "top-hat" profiles (Mallinson, *et al.*, 1999), (Lee and Goldstein, 2002), (Smith and Glezer, 1998) are obtained. However, for the lowest pressure amplitude, the synthetic jet expansion is more rapidly affected by dissipation effects as it can be seen in figure 6c.
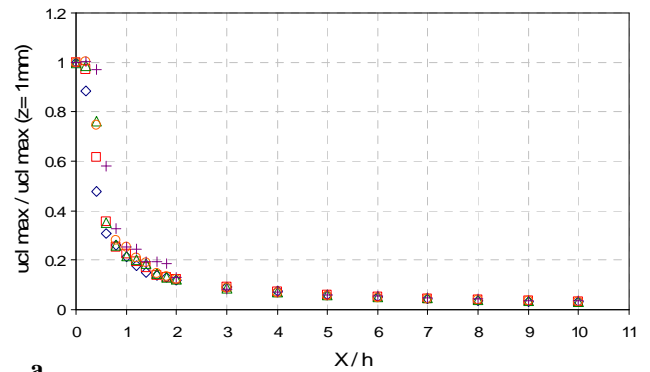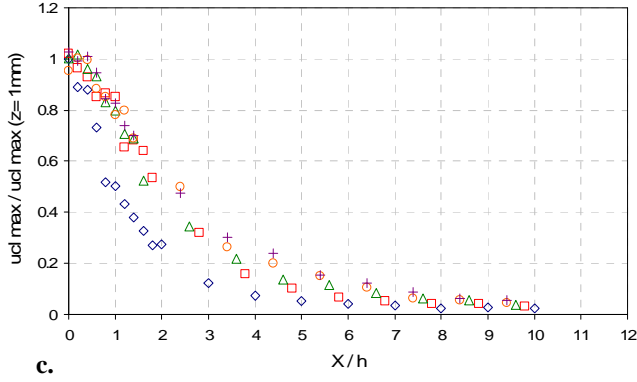

a.
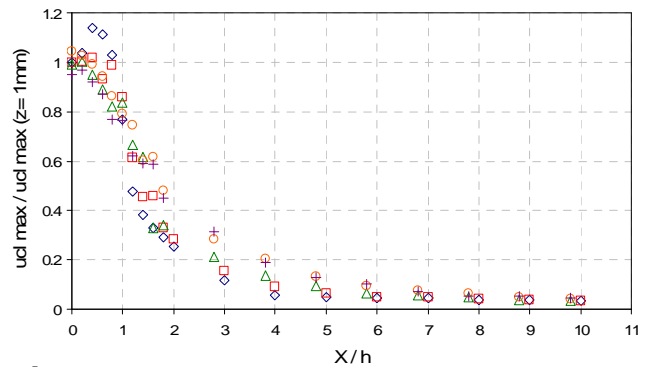
b.

Figure 6. Distribution of maximum velocity above the SJA. f = 200 Hz   a. z = 1,   b. z= 3,   c. z=5 mm.
◇: 250 Pa, □: 500 Pa, △: 1000 Pa, ○: 1500 Pa, +: 2000 Pa

NUMERICAL MODEL OF THE SJA

Numerical models of the synthetic jet actuator have been developed using the finite-volume solver Fluent. A laminar model and two turbulence models based on the Reynolds Average approach were tested:

• the Realizable k-ε model which is more capable to accurately predict the spreading rate of both planar and round jets than the standard or RNG models proposed in Fluent;

• the standard k-ω model, chosen for its ability to take into account low Reynolds number effects, compressibility effects, and shear flow spreading.

All cases are solved with a 2nd order upwind discretization scheme, and the SIMPLEC algorithm is used for pressure-velocity coupling. Further details about the numerical models (grid size, time step, boundary conditions type,…) can be found in a previous paper (Batikh, *et al.*, 2006).

Experimental data are compared to the numerical ones for the following configuration: 1100 Hz actuation frequency and 2×10^3 Pa pressure amplitude in the cavity. Figure 7 shows the distribution of the maximum velocity along the jet centerline obtained from hot-wire measurements compared to the numerical simulations data obtained with the three viscous models.
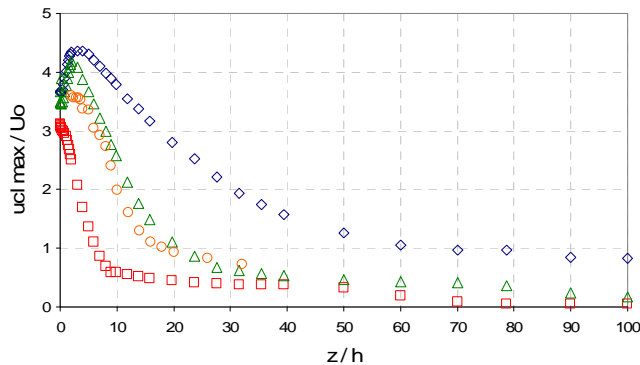

Figure 7. Distribution of maximum velocity on the jet axis – comparison between experimental and numerical data
f = 1100 Hz, h = 500 µm, pressure amplitude : 2×10^3 Pa
◇: Laminar, □: k-ε, △: k-ω, ○: Experimental

Experimental data are in good agreement with the *k-ω* turbulent model.

The main experimental synthetic jet parameters are reported in table 1. The experimental Stokes number is very close to the one chosen for the numerical simulations, confirming that this experimental configuration can be used for the validation of the numerical models. Experimental values of Reynolds and Strouhal numbers are here closer to the numerical values obtained from the k-ε model. This trend is confirmed in figure 8 which presents the velocity magnitude distribution at z/h = 10.

Model	L_0 (m)	U_0 (m/s)	Re_{U0}	$U_{j\,max}$ (m/s)	St	Sr
Laminar	0.01223	13.9	477	51	11.08	0.2568
Turbulent k-ε	0.01096	12.5	428	39	11.08	0.2866
Turbulent k-ω	0.01240	14.1	484	49	11.08	0.2533
Exp	0.011	12.5	428	45	10.88	0.2765

Table 1. Main parameters for the experimental SJA

Further experimental investigation is necessary for the validation of the numerical model. In particular, it was not possible to obtain from a single hot-wire the velocity components across the jet which would have permitted to get the cross-stream and stream-wise velocity profiles. In a future work, PIV measurements will be performed in order to explore the jet more in details. However, according to the preceding results, the k-ε model has been chosen for the first simulations of the interaction between the SJA and a cross wall flow.

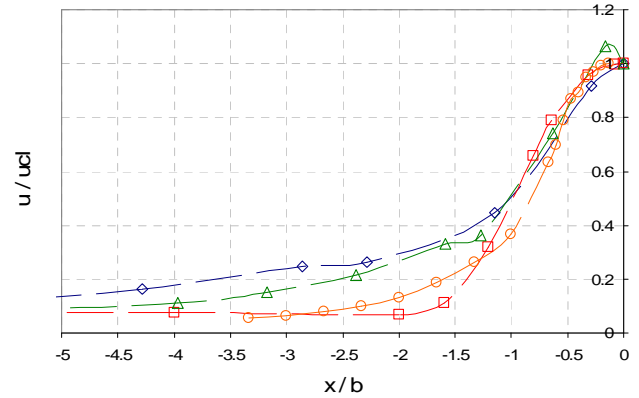**Figure 8.** Distribution of time-averaged velocity at z/h = 10 with f = 1100 Hz, h = 500µm, pressure amplitude : 2×10^3 Pa
◇: Laminar, □: k-ε, △: k-ω, ○: Experimental

Additional information about the flow structure (vorticity contours, velocity vectors map,…) can be found in (Batikh, *et al.*, 2006). However, Figure 9 shows the iso-contours of vorticity at two different times: t/T = 0.25 and t/T = 0.75 corresponding respectively to the middle of the blowing phase and of the suction phase.

Vortices are generated at the slot at the beginning of the ejection phase. However, once detached from the slot they rapidly merge with the preceding pair of vortices (figure 9-b) which leads to the generation of an unique pair of vortices of higher size. Dissipation occurs quite rapidly due to turbulence and the big vortices pair remains nearly stationary during the cycle. In each part of the cavity, only two circulation cells are generated and distorted according to the piston motion during the working cycle.
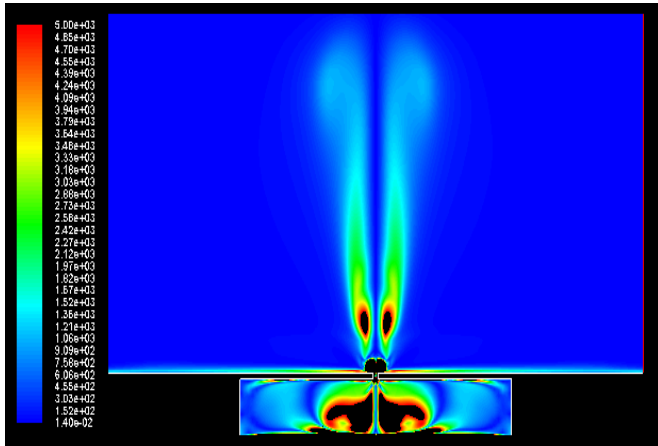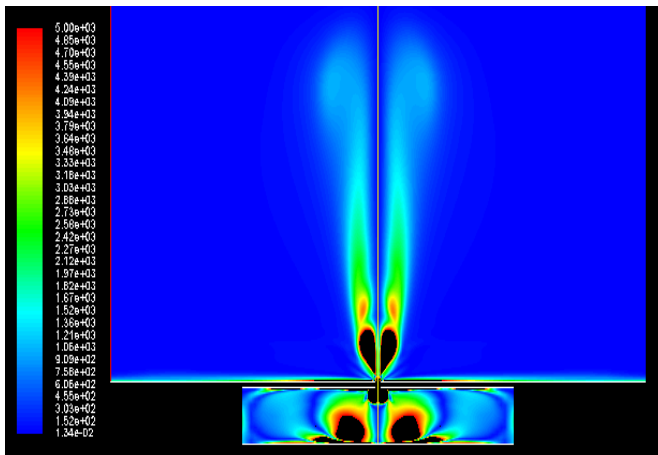

Figure 9. Iso-contours of vorticity – k-ε model. a) $t/T = 0.25$, b) $t/T = 0.75$

## CHARACTERIZATION OF THE WALL FLOW WITHOUT SJA

Before to test the effect of the SJA on the cross flow, the wall jet has first been characterized.

Figure 10-a shows three velocity profiles in the symmetry plane of the jet ($y = 0$) at various distances from the rectangular channel exit ($x = 3, 60, 120$ mm). Even if the velocity profile is not as uniform as expected just downstream the channel exit ($x = 3$ mm), the boundary layer and the mixing layer are rapidly growing leading to classical wall jet profile at $x = 60$ mm.

The symmetry of the jet with respect to the plane $y = 0$ is also well checked in the Figure 10-b which shows the velocity profiles at $z = 5$ mm, for the three values of x (3, 60 and 120 mm).
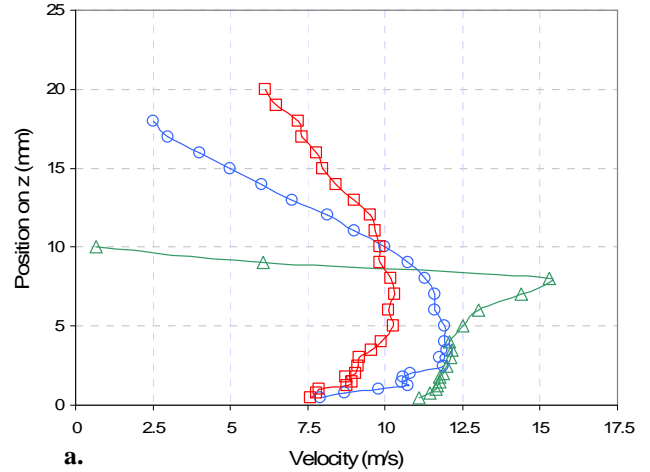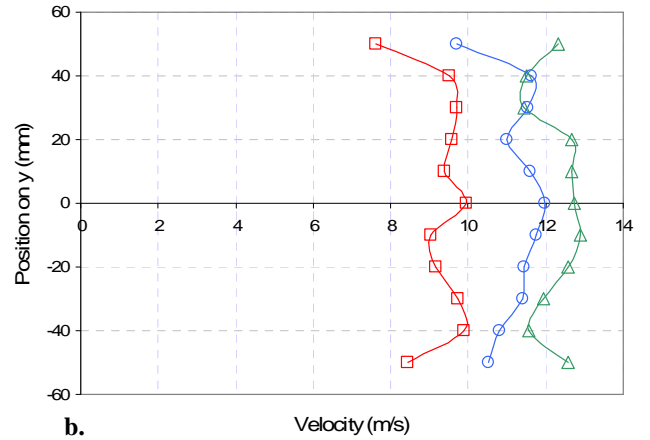
Figure 10. Wall jet velocity profiles for 3 sections
a) z profile, b) y profile
Δ: 3mm, O: 60 mm, □: 120mm

SYNTHETIC JET WITH CROSS FLOW

Measurements have been done for two values (11.5 m/s and 6.5 m/s) of the "uniform" (or freestream) velocity U_∞ of the cross flow just upstream from the SJA ($x = 90$ mm). This can be checked at x=90mm in figures 11 and 12. The SJA is positioned at $x = 97$ mm (figure 2 a) and actuated at $f = 200$ Hz.

For each configuration, 10 time-average velocity profiles were recorded : the first one just upstream from the SJA (x = 90 mm), the second one at the position of the SJA and 8 profiles downstream from the SJA ($x = 98, 99, 100, 105, 110, 115, 120$ and 125mm).

Table 2 summarizes the main experimental parameters of the two tested configurations.

Case	U_∞ (m/s)	$Re_\infty = \rho_\infty U_\infty / \mu_\infty$	U_{jmax}/U_∞	Re_{U0}	$C\mu$
1	11.5	7872	1.43	565	5.10^{-3}
2	6.5	4450	2.5	565	0.0184

Table 2. Main parameters for the SJA with cross flow experimental configurations

Figures 11 and 12 show the velocity profiles at each position with and without SJA actuation for cross flow "uniform" velocities of respectively 11.5 and 6.5 m/s.
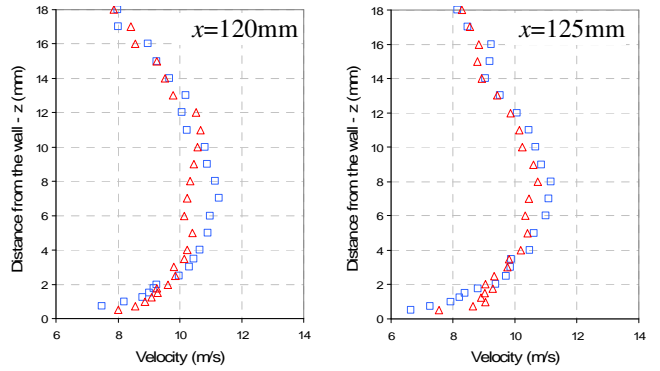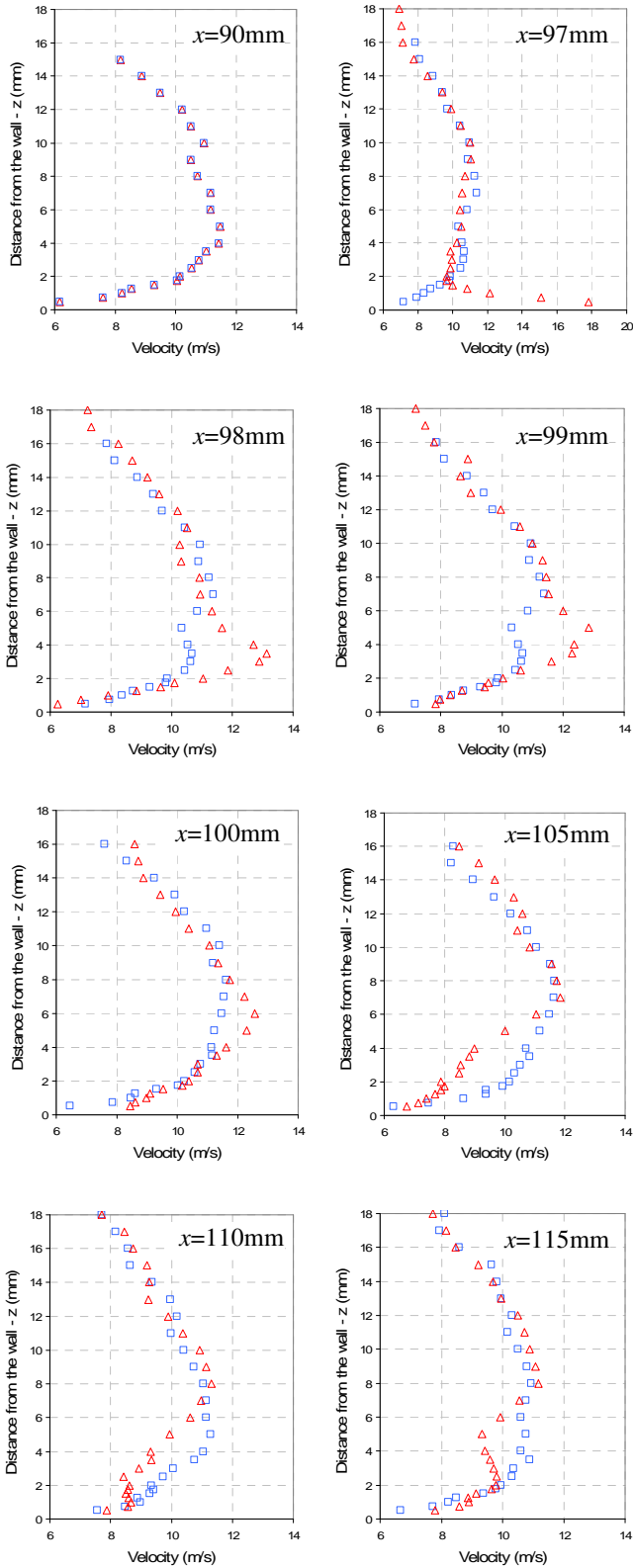

Figure 11. Velocity profiles with (on) and without (off) actuation of SJA – Cross flow velocity : 11.5 m/s
△: SJ-On, □: SJ-Off

The effects of the SJA on the boundary layer of the cross flow are clearly visible on these profiles (figure 11). At the slot level, the velocity magnitude is strongly increased for z < 2 mm. This is mainly due to the vertical component of the synthetic jet velocity at the slot exit. It was not possible indeed to identify z and y components of the velocity with a single hot wire probe. Nevertheless, it can be seen that the synthetic jet is bended by the cross flow : the z position of the interaction zone is increasing, moving downstream from the SJA position up to x = 100 mm. On the following profiles, the flow velocity is reduced, mainly in the boundary layer, when the SJA is switched on. This is due to the presence a recirculation zone created by the "right" vortices generated by the SJA and convected downstream by the cross flow. This phenomena apparition is dependent on the ratio between the synthetic jet maximum velocity at the slot exit plane and the cross flow free stream velocity. In their numerical study, Mittal (Mittal, *et al.*, 2001) have observed this behaviour for a velocities ratio around 3 which is also the case in our configuration ($U_{jmax}/U_{\infty} \approx 36 / 11.5 \approx 3$). Finally, from x = 120 mm, the flow modifications due to the synthetic jet actuation become negligible.

Globally, the same behaviour is observed when the wall jet free stream velocity is 6.5 m/s (figure 12). However, as the momentum coefficient is more than three times higher than in the previous configuration (cf. table 2), the effects are more emphasized. The synthetic jet penetration in the cross flow is more important : the velocity profile near the wall is strongly modified up to z = 8 mm (for x = 100 mm). On the other hand, its deviation from the vertical position is slighter.

Moreover, as the synthetic jet momentum is stronger compared to the wall jet one, the "left" vortices generated at the slot exit are here not completely cancelled by the cross flow but they induce an increase of the cross flow velocity more far away from the wall which can be observed from x = 105 mm up to x = 120 mm.

As the jet is less bended by the cross flow, the recirculation zone clearly observed in the previous configuration seems here to be much more reduced. However, as the hot-wire does not give information on the velocity direction, this analysis has to be confirmed thanks to PIV measurements which will soon be performed on this experimental setup.
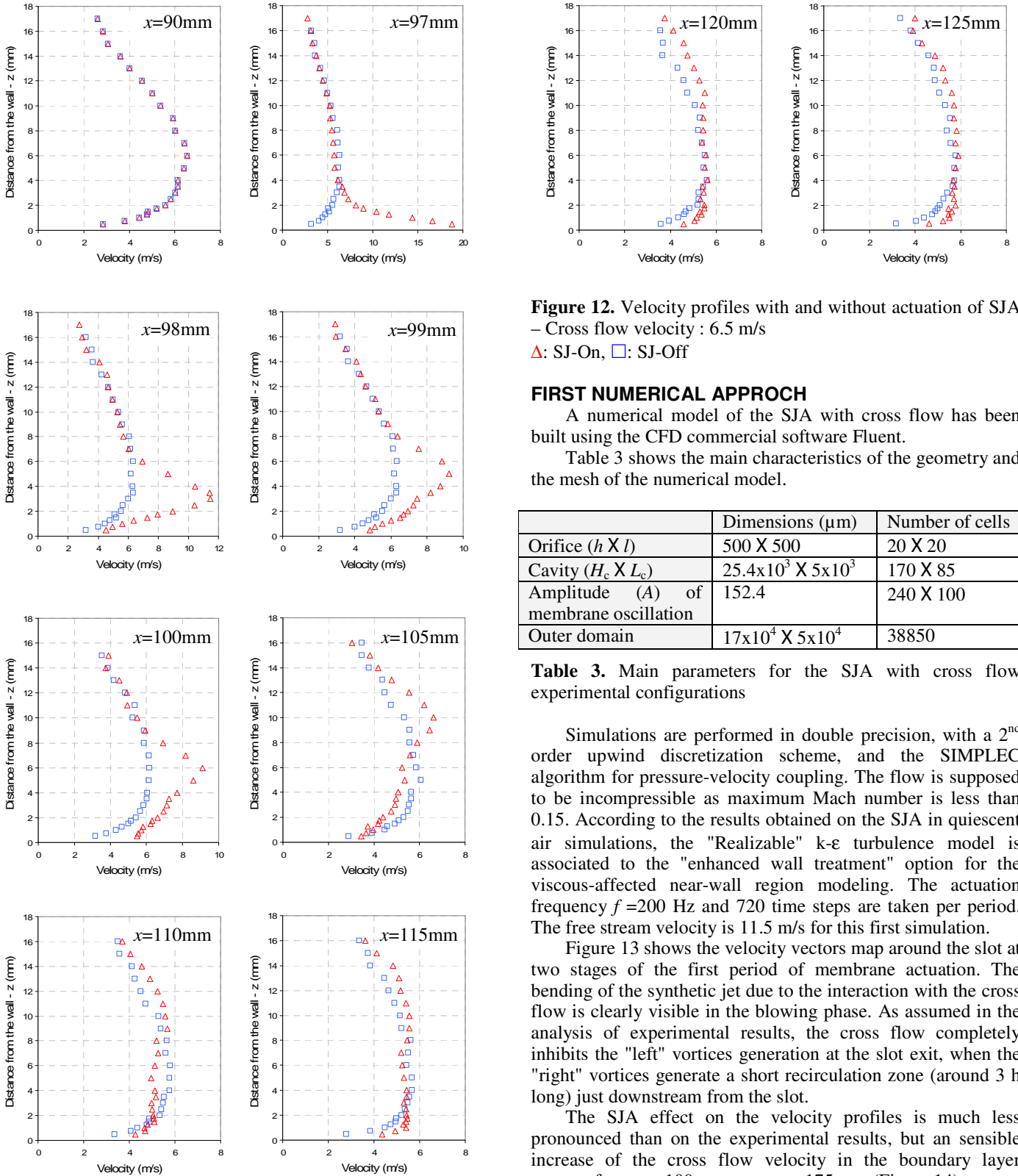
Figure 12. Velocity profiles with and without actuation of SJA – Cross flow velocity : 6.5 m/s

Δ: SJ-On, ☐: SJ-Off

FIRST NUMERICAL APPROCH

A numerical model of the SJA with cross flow has been built using the CFD commercial software Fluent.

Table 3 shows the main characteristics of the geometry and the mesh of the numerical model.

	Dimensions (μm)	Number of cells
Orifice (h ✗ l)	500 ✗ 500	20 ✗ 20
Cavity (H_c ✗ L_c)	25.4×10^3 ✗ 5×10^3	170 ✗ 85
Amplitude (*A*) of membrane oscillation	152.4	240 ✗ 100
Outer domain	17×10^4 ✗ 5×10^4	38850

Table 3. Main parameters for the SJA with cross flow experimental configurations

Simulations are performed in double precision, with a 2nd order upwind discretization scheme, and the SIMPLEC algorithm for pressure-velocity coupling. The flow is supposed to be incompressible as maximum Mach number is less than 0.15. According to the results obtained on the SJA in quiescent air simulations, the "Realizable" k-ε turbulence model is associated to the "enhanced wall treatment" option for the viscous-affected near-wall region modeling. The actuation frequency f =200 Hz and 720 time steps are taken per period. The free stream velocity is 11.5 m/s for this first simulation.

Figure 13 shows the velocity vectors map around the slot at two stages of the first period of membrane actuation. The bending of the synthetic jet due to the interaction with the cross flow is clearly visible in the blowing phase. As assumed in the analysis of experimental results, the cross flow completely inhibits the "left" vortices generation at the slot exit, when the "right" vortices generate a short recirculation zone (around 3 h long) just downstream from the slot.

The SJA effect on the velocity profiles is much less pronounced than on the experimental results, but an sensible increase of the cross flow velocity in the boundary layer appears from x = 100 mm up to x = 175 mm (Figure 14).

These first numerical results are not completely coherent with the experimental data presented in the previous chapters. However, due to the size of the mesh and the very low time step, the simulations are very long : one week for the

simulation of one actuation period using a PC with a double AMD processor running at 2.6 GHz. When writing this paper, only the first period had been calculated. The numerical simulation was thus still in its transient phase: for the simulations of the SJA in quiescent air, five actuation periods were indeed necessary before obtaining a stationary solution. Further simulations should thus permit to obtain averaged numerical velocity profiles which could be compared to experimental results.
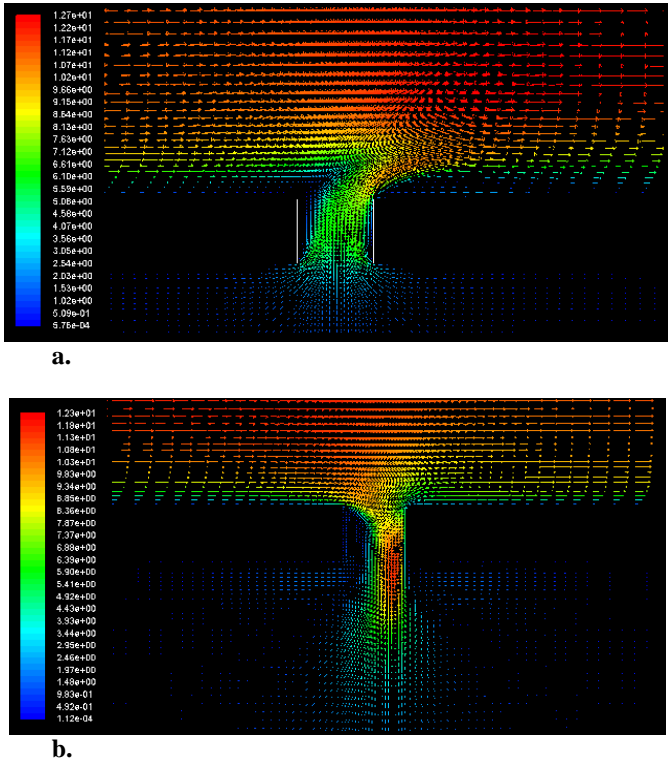

a.

b.

Figure 13. Velocity vectors map around the slot a) $t/T = 0.25$ (blowing) b) $t/T = 0.75$ (suction)

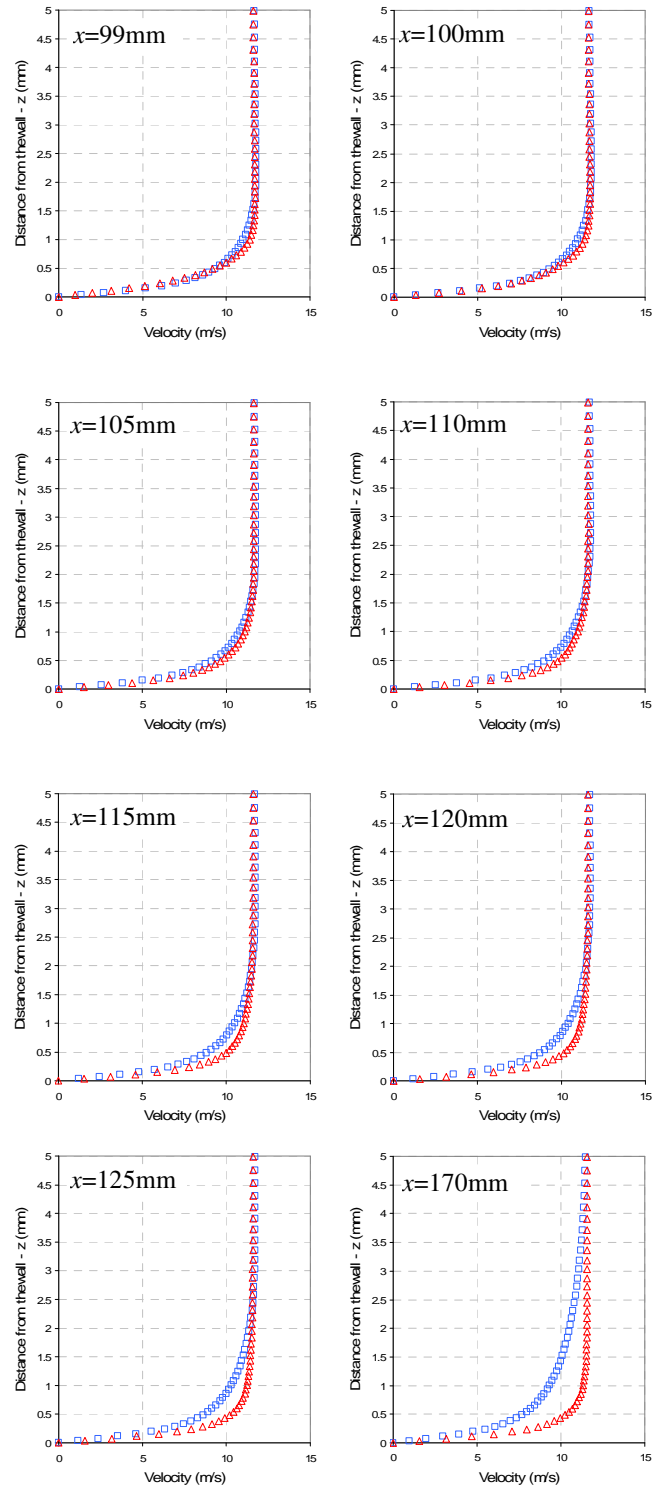**Figure 14.** Numerical velocity profiles with and without actuation of SJA – Cross flow velocity : 11.5 m/s
Δ: SJ-On, □: SJ-Off

CONCLUSION

Experimental characterization of a Synthetic Jet Actuator in a cross wall jet flow has been performed for two free stream velocities of the cross flow, using hot-wire anemometry. The effect of the synthetic jet is clearly visible on the velocity

9   Copyright © #### by ASME

profiles downstream from the slot and all the more pronounced that the velocity ratio and the jet momentum coefficient are important.

A numerical model of this experimental configuration has been developed on the CFD software Fluent. First numerical results confirm some of the experimental observations: jet bending under the cross flow action, recirculation zone apparition just downstream from the SJA…However, further simulations are needed to reach a stationary state of the flow permitting a full comparison with the experimental data. In the same time, Particle Image Velocimetry will be performed in order to complete the experimental data bank, since hot-wire measurements do not give complete information on the velocity directions around the SJA slot.

REFERENCES

Batikh A., Baldas L., Caen R., and Colin S., Contrôle actif en aérodynamique au moyen de Micro actionneurs fluidiques, *2ème Congrès Français de Microfluidique - Microfluidique 2004 (μFlu'04)*, Toulouse - France, 2004.

Batikh A., Caen R., Colin S., Baldas L., Kourta A., and Boisson H.-C., Numerical and experimental study of micro synthetic jets for flow control, *3rd Microfluidics French Conference - Microfluidics 2006 (μFlu'06)*, Toulouse - France, 2006.

Gad El Hak M., Modern developments in flow control, *Applied Mechanical Review*, vol. 49, pp.365-379, 1996

Greenblatt D., Paschal K. B., Yao C.-S. and Harris J., Experimental Investigation of Separation Control Part 2: Zero Mass-Flux Oscillatory Blowing, *AIAA Journal*, Vol. 44, N° 12, 2006

Ho C.-M. and Tai Y.-C., Microelectromechanical systems (MEMS) and fluid flows, *Ann. Rev. Fluid Mech,* vol. 30, pp. 579-612, 1998.

Kral L. D., Donovan J. F., Cain A. B., and Cary A. W., Numerical simulations of synthetic jet actuators, *AIAA Paper* 97-1824, 1997.

Lee C. Y. and Goldstein D. B., Two-dimensional synthetic jet simulation, *AIAA Journal,* vol. 40, 2002.

Mallinson S. G., Hong G., and Reizes J. A., Some characteristics of synthetic jets, *AIAA Paper* 99-3651, 1999.

Mittal R., Rampunggoon P. and Udaykumar H. S., Interaction of a Synthetic Jet with a Flat Plate Boundary Layer, *AIAA Paper* 2001-2773, 2001

Seifert A. and Pack L. G., Oscillatory Control of Separation at High Reynolds Numbers, *AIAA Journal*, Vol. 37, N° 9, 1999.

Smith B. L. and Glezer A., The formation and evolution of synthetic jets, *Phys. Fluids,* vol. 10, pp. 2281-2297, 1998.

Traub L. W., Gilarranz J. L., and Rediniotis O. K., Delta wing control via Synthetic Jet Actuator, *AIAA Paper* 2002-0415*, 2002.

Utturkar Y., Holman R., Mittal R., Carroll B., Sheplak M., and Cattafesta L., A jet formation criterion for synthetic jet actuators, *41st Aerospace Sciences Meeting and Exhibit,* Reno, Nevada: 2003-0636, 2003.

Wu K. E. and Breuer K. S., Dynamics of Synthetic Jet Actuator Arrays for Flow Control, *33rd AIAA Fluid Dynamics Conference and Exhibit,* Orlando, Florida: AIAA 2003-4257, 2003.